Klebsiella aerogenes UreF: Identification of the UreG Binding Site and Role in Enhancing the Fidelity of Urease Activation

ARTICLE *in* BIOCHEMISTRY · MARCH 2012

Impact Factor: 3.02 · DOI: 10.1021/bi3000897 · Source: PubMed

2 AUTHORS, INCLUDING:

Robert P Hausinger
Michigan State University
179 PUBLICATIONS **9,590** CITATIONS

Published in final edited form as:
Biochemistry. 2012 March 20; 51(11): 2298–2308. doi:10.1021/bi3000897.

Klebsiella aerogenes UreF: Identification of the UreG Binding Site and Role in Enhancing the Fidelity of Urease Activation[†]

Jodi L. Boer[‡] and **Robert P. Hausinger**[‡,§,*]

[‡]Department of Biochemistry & Molecular Biology, Michigan State University, East Lansing, Michigan 48824

[§]Department of Microbiology & Molecular Genetics, Michigan State University, East Lansing, Michigan 48824

Abstract

The Ni-containing active site of *Klebsiella aerogenes* urease is assembled through the concerted action of the UreD, UreE, UreF, and UreG accessory proteins. UreE functions as a metallochaperone that delivers Ni to a complex of UreD—UreF—UreG bound to urease apoprotein, with UreG serving as a GTPase during enzyme activation. The present study focuses on the role of UreF, previously proposed to act as a GTPase activating protein (GAP) of UreG. Sixteen conserved UreF surface residues that may play roles in protein:protein interactions were independently changed to Ala. When produced in the context of the entire urease gene cluster, cell-free extracts of nine site-directed mutants had less than 10% of the wild-type urease activity. Enrichment of the variant forms of UreF, as the UreE-F fusion proteins, uniformly resulted in co-purification of UreD and urease apoprotein; whereas UreG bound to only a subset of the species. Notably, reduced interaction with UreG correlated with the low activity mutants. The affected residues in UreF map to a distinct surface on the crystal structure, defining the UreG binding site. In contrast to the hypothesis that UreF is a GAP, the UreD—UreF—UreG—urease apoprotein complex containing K165A UreF exhibited significantly greater levels of GTPase activity than that containing the wild-type protein. Additional studies demonstrated the UreG GTPase activity was largely uncoupled from urease activation for the complex containing this UreF variant. Further experiments with these complexes provided evidence that UreF gates the GTPase activity of UreG to enhance the fidelity of urease metallocenter assembly, especially in the presence of the non-cognate metal Zn.

Urease, an enzyme that is widely found in bacteria, plants, and fungi, hydrolyzes urea into ammonia and carbonic acid, with the resulting ammonification and increase in pH having important implications in medicine and agriculture (1–4). The best-studied urease system is produced by recombinant *Escherichia coli* expressing the *Klebsiella aerogenes* urease genes, *ureDABCEFG*. *K. aerogenes* urease contains three subunits, UreA, UreB, and UreC, that form a trimer of trimers in the supramolecular structure (5). The three active sites in the native enzyme each contain two Ni atoms bridged by a lysine carbamate and are deeply buried in the protein. Assembly of these active sites requires nickel, bicarbonate, GTP

[†]These studies were supported by the National Institutes of Health (DK045686)

[*]To whom correspondence should be addressed: Biomedical Physical Sciences, 567 Wilson Road, Room 2215, Michigan State University, East Lansing, MI 48824. Telephone: (517) 884-5404. Fax: (517) 353-8957. hausinge@msu.edu.

Supporting information

This file contains a table listing the oligonucleotides used to create the site-directed mutations, a table of urease activities in cell-free extracts of *ureF* mutants (that identifies the corresponding residues in *K. aerogenes* and *H. pylori*), and an alignment of selected UreF sequences. This material may be accessed free of charge online at http://pubs.acs.org.

hydrolysis, and products of the other four *ure* genes (2, 4). The $(UreABC)_3$ apoprotein can be purified alone (6) or with combinations of the UreD, UreF, UreG, and UreE accessory proteins (7–11). With each additional accessory protein, $(UreABC)_3$ is more primed for activation, leading to greater *in vitro* activity after incubation with Ni, bicarbonate, and GTP when UreG is present (Figure 1). As summarized below, some properties of these complexes and the individual urease accessory proteins have been discerned (these comments refer to the *K. aerogenes* urease components unless stated otherwise); however, their exact roles remain unclear.

The $(UreABC—UreD)_3$ complex has UreD bound at the vertices of the triangular apoprotein according to small-angle X-ray scattering (SAXS) (12) and chemical cross-linking (13) approaches. When *ureD* is expressed alone the resulting protein is insoluble, but a fusion of the maltose binding protein (MBP) with UreD is soluble and functional (14). Surprisingly, the fusion protein does not bind to $(UreABC)_3$ *in vitro*, but it forms a complex with the urease apoprotein when co-produced *in vivo*. Also of interest, MBP-UreD binds divalent metal ions (~2.5 Ni per protomer, K_d ~50 μM; ~4 Zn per protomer, K_d ~5 μM). The structure of UreH (a UreD homologue) from *H. pylori* was recently reported as part of a $(UreH—UreF)_2$ complex (15). UreH exhibits a novel fold consisting of 17 β-strands and 2 α-helices. The working hypothesis for urease activation suggests that UreD enhances the activation efficiency of urease apoprotein while also acting as a scaffold for the binding of the other auxiliary proteins (2, 4).

$(UreABC—UreD—UreF)_3$ represents the apoprotein with heterodimers of UreD—UreF binding at its vertices, according to SAXS analysis (12). Chemical cross-linking studies indicate a conformational change takes place in the urease apoprotein within this complex and show a link between UreB and UreF (13). Yeast 2-hybrid experiments carried out using the *H. pylori* and *Proteus mirabilis* proteins also support an interaction between UreF and UreD/H (16, 17). Although *K. aerogenes* UreF is insoluble when produced alone, the fusion proteins with UreF linked to MBP (18) or to UreE (creating UreE-F) (19) are soluble. The gene encoding the fusion protein complements a *ureF* deletion mutant and binds *in vitro* to UreABC—UreD or MBP-UreD (14, 19). Truncation variants indicate that the C-terminal 15 residues of UreF are essential for forming the activation complex, and the N-terminal 24 residues are needed for urease activation, but not for binding to the activation complex (19). The crystal structure was solved for truncated *H. pylori* UreF lacking its C-terminal 21 residues and with its first 24 residues disordered (20). The *H. pylori* $(UreH—UreF)_2$ structure contains the last 21 residues that the structure of UreF alone was missing, but the UreF N-terminus also was unstructured in this complex (15). The dimeric UreF protein exhibits an all-alpha-helical fold with highly conserved residues mapping to one face. Notably, the dimer interface would need to be disrupted to form $(UreABC—UreD—UreF)_3$. A modeling study suggested a role of UreF as a GTPase activating protein (GAP) for UreG, a small GTPase (21).

UreABC—UreD—UreF—UreG is formed by UreG binding to the above complex or, as likely to occur in the cell, by UreD—UreF—UreG binding to the urease apoprotein. The UreABC—UreD—UreF—UreG complex was shown to have increased urease activation potential when incubated with Mg_2GTP in addition to Ni and bicarbonate (10). A related complex is produced by utilizing the *Strep II*-tagged version of UreG ($UreG_{Str}$) to purify UreABC—UreD—UreF—$UreG_{Str}$ (22). UreG itself is soluble and has been characterized from several organisms. In *K. aerogenes* this protein is a monomer that binds one Ni or one Zn with K_d values of about 5 μM (22). UreGs from other microorganisms have slightly different properties. *H. pylori* UreG dimerizes when Zn is bound, but remains monomeric when Ni is present or in the absence of metal ion (23). UreG proteins from *Bacillus pasteurii* and *Mycobacterium tuberculosis* are dimeric with the subunits joined by a disulfide bridge

(24, 25). All UreGs contain GTPase-specific motifs including a P-loop, which is necessary for GTP binding, but low or undetectable GTPase activity is found for the isolated proteins, consistent with nucleotide hydrolysis being coupled to urease activation in the larger complex.

UreE is proposed to be the metallochaperone responsible for delivering Ni to the activation complex to allow for maturation of the active site (26). A complex containing all of the urease proteins has been detected (12, 22). Furthermore Ni or Zn promotes binding between UreE and UreG (22), as also noted with the *H. pylori* proteins (27).

Here we examine the effects of UreF variants on urease activity, the interactions of UreF with other urease proteins, and the function of UreF in urease activation. Variant forms of UreF were created on the basis of the *H. pylori* UreF structure and sequence alignments. The competence of each variant protein was assessed for *in vivo* activation of urease. Pull-down analysis of UreE-F constructs was carried out to test the effects of the mutations on *in vivo* and *in vitro* interactions with other urease components. Finally, the properties of UreABC—UreD—UreF—UreG$_{Str}$ and a key UreF variant complex were characterized, the proposed role of UreF as a GAP was assessed, and an alternative hypothesis that UreF functions as a checkpoint for proper metallocenter synthesis was examined.

EXPERIMENTAL PROCEDURES

Plasmids, oligonucleotides, and site-directed mutagenesis

A description of the plasmids used in this study is provided in Table 1, and oligonucleotides used here are identified in supplementary material as Table S1. Plasmids pKK17 (encoding the complete *ureDABCEFG* gene cluster) (26), pKKEF (with the UreE-F fusion protein encoded within the complete urease gene cluster), and pET-EF (encoding a translational fusion of UreE and UreF) (19) were mutated by using overlapping oligonucleotides containing the desired mutations and *Pfu*Turbo Hotstart PCR mastermix (Promega). The products were digested using *Dpn*1 and transformed into chemically competent *E. coli* DH5α cells (Invitrogen). The mutations were confirmed by sequencing (Davis Sequencing, CA), the pET-EF based plasmids were transformed into C41(DE3) competent cells (28), and all other plasmids were transformed into BL21 (DE3) competent cells. In order to examine further the K165A mutation of UreF, plasmid pKK17-K165A was digested with AatII and AvrII and the desired fragment was ligated into similarly digested pKKG (expressing the *Strep II*-tagged version of UreG along with the other urease genes) (22) to create pKKG-UreF-K165A. The same restriction enzymes were used to replace a fragment of pEC005 (containing *ureFG* cloned into pACT3) (14) with the DNA encoding the K165A mutation, producing pEC005-UreF-K165A. A DNA fragment encoding UreG T21A was inserted into both pKKG and pEC005 by using AatII and RsrII, forming pKKG-T21A and pEC005-UreG-T21A. Plasmids pKAUD2, pIBA3+UreG, and pEC002, used for production of (UreABC-UreD)$_3$, UreG$_{Str}$, and MBP-UreD—UreF—UreG, were described previously (7, 14, 22).

Protein purification

E. coli C41(DE3) cells producing UreE-F or its variations were grown overnight in 10 mL lysogeny broth (LB) supplemented with 300 μg mL^{-1} ampicillin. The cultures were used to inoculate 1 L of Terrific Broth (TB, Fisher BioReagents) supplemented with 300 μg mL^{-1} ampicillin, grown to optical densities at 600 nm (OD$_{600}$) of 0.4 to 0.6, induced with 0.5 mM isopropyl β-D-1-thiogalactopyranoside (IPTG), and grown overnight at 37 °C. Cells were harvested by centrifugation, resuspended (1 g mL^{-1}) in buffer A (20 mM Tris, pH 7.8, containing 500 mM NaCl and 60 mM imidazole), supplemented with 1 mM phenylmethyl-

sulfonyl fluoride, and sonicated (Branson 450 sonifier, five repetitions of 2 min each at 3 W output power and 50% duty cycle). Disrupted cells were centrifuged at 100,000 × *g* at 4 °C for one h and the cell-free supernatants were loaded onto a 5 mL Ni-nitrilotriacetic acid (NTA) column equilibrated with buffer A. The column was washed with buffer A until the A_{280} reached baseline, and bound proteins were eluted by using buffer B (20 mM Tris, pH 7.8, containing 500 mM NaCl and 1 M imidazole). Fractions containing UreE-F or its variations were combined and dialyzed overnight into 20 mM Tris, pH 7.8, containing 100 mM NaCl, 1 mM EDTA and 1 mM dithiothreitol (DTT). The proteins were further purified by gel filtration chromatography using a Superdex-75 column (65 cm × 2.0 cm diameter; GE Healthcare) equilibrated in the same buffer.

E. coli cells producing UreABC—UreD—UreF—$UreG_{Str}$ or its variants were grown overnight in 10 mL LB supplemented with 300 μg mL^{-1} ampicillin. The cultures were used to inoculate 1 L of LB containing 300 μg mL^{-1} ampicillin, grown to an OD_{600} of 0.4 to 0.6, induced with 0.1 mM IPTG, and grown overnight at 37 °C. Cells were harvested by centrifugation, resuspended in buffer W (100 mM Tris pH 8.0, 150 mM NaCl, 1 mM EDTA), and sonicated (same protocol as above). Disrupted cells were centrifuged at 100,000 × *g* at 4 °C for one h and the cell-free supernatant was loaded onto a *Strep*-tactin column. The column was washed with buffer W until the A_{280} was at baseline, and bound proteins were eluted with the same buffer containing 2.5 mM desthiobiotin. Fractions containing the protein of interest were concentrated and loaded onto a Superdex-200 column equilibrated with 25 mM 4-(2-hydroxyethyl)-1-piperazineethanesulfonic acid (HEPES) buffer, pH 7.4, containing 150 mM NaCl and 1 mM tris(2-carboxyethyl)phosphine (TCEP). Before use in further assays, the protein was dialyzed into buffer with no TCEP.

$(UreABC—UreD)_3$ and $UreG_{Str}$ were produced using pKAUD2 and pIBA3+UreG, respectively, and purified as previously described (7, 22). MBP-UreD—UreF—UreG was obtained from cells coexpressing pEC005 and pEC002 (14) and isolated as reported earlier (29).

Sodium dodecyl sulfate (SDS)-polyacrylamide gel electrophoresis (PAGE)

SDS-PAGE was performed by using standard buffers (30), 12% acrylamide running gels, and 4% stacking gels, except in the case of UreABC—UreD—UreF—$UreG_{Str}$ analysis, when 15% running gels were used.

Pull-down assays using cell-free extracts

Cells containing pKKEF and its variants were grown in 50 mL TB supplemented with ampicillin (300 μg mL^{-1}) to an OD_{600} of 0.4 to 0.6, induced with 0.5 mM IPTG, and allowed to grow overnight at 37 °C. Cells were harvested, resuspended in 2 mL buffer A, sonicated, and microcentrifuged (14,000 rpm). Cell-free extracts were added to 200 μL of Ni-NTA resin, washed with 5 mL buffer A, and then eluted with 250 μL buffer B. Eluted fractions were examined for the presence of other urease related proteins by using 15% SDS-PAGE.

In vitro pull-down assays

Two distinct types of *in vitro* pull-down studies were carried out. (i) UreE-F and its variants were tested for their abilities to bind to purified $(UreABC—UreD)_3$. The apoprotein complex (12 μM nascent active site, dialyzed into buffer containing 20 mM Tris, pH 7.8, and 100 mM NaCl) was combined with UreE-F and its variants (12 μM protomer concentration in the same buffer) and incubated at room temperature for 20 min. The protein mixtures were applied to 0.5 mL Ni-NTA columns, washed with 5 mL of 20 mM Tris, pH 7.8, containing 100 mM NaCl, and eluted with the same buffer containing 1 M imidazole.

(ii) For examining interactions of UreF with UreG, samples of UreE-F or its site-directed variants were combined with purified $UreG_{Str}$ (12 μM of each protomer) in 20 mM Tris, pH 7.8, buffer and incubated for one h at 42 °C. The proteins were applied to 0.5 mL *Strep*-Tactin columns, washed with 5 mL of 20 mM Tris buffer and eluted with 2 mM desthiobiotin in the same buffer. Each *in vitro* pull-down assay was analyzed by 12% SDS-PAGE and gel scanning (Alpha Imager 2200), with the intensities of the bands divided by the molecular mass of each protein (MBP-UreD, 72.9 kDa; UreC, 60.3 kDa; UreE-F, 42.8 kDa; UreD, 29.8 kDa; UreF, 25.2 kDa; $UreG_{Str}$, 23.2 kDa; UreG, 21.9 kDa; UreB, 11.7 kDa; and UreA, 11.1 kDa; though UreA and UreB typically were not included in the calculations due to the aberrant dye-binding behavior of these small subunits) to assess the ratios of interactions.

Urease activity and protein assays

Urease activities were measured by quantifying the rate of ammonia release from urea by formation of indophenol, which was monitored at 625 nm (31). One unit of urease activity is defined as the amount of enzyme required to hydrolyze 1 μmole of urea min^{-1} at 37 °C. The standard assay buffer contained 50 mM HEPES, pH 7.8, and 50 mM urea. Protein concentrations were determined by a commercially available protein assay (Bio-Rad).

Urease activation assays

UreABC—UreD—UreF—$UreG_{Str}$ and its variants were activated for one h at 37 °C in a standard solution containing 100 mM HEPES buffer, pH 8.3, containing 150 mM NaCl, 100 μM $NaHCO_3$, 100 μM $NiCl_2$, and the indicated amounts of GTP (provided as its Li salt with two equivalents of Mg), unless otherwise noted. Experiments to examine the effects of Zn in the activation solution used the concentrations indicated in the figures. After activation, urease activity was measured by using the standard assay, except that the buffer additionally contained 0.5 mM EDTA to prevent Ni-dependent inhibition. Time course experiments were analyzed by using Sigma Plot (Systat Software, Inc.) and the following equation, where Y is the measured urease activity in U/mg, A_{max} is the maximal urease activity generated, t is the time in minutes, and $t_{1/2}$ is the time needed to reach half of the maximal activity.

$$Y = A_{max} t/(t_{1/2}+t) \quad (1)$$

Statistically significant differences in urease activation were determined by a p value < 0.05 when using the Student's t-test.

GTPase activity assays

GTPase activity was measured by monitoring the amount of released phosphate using malachite green (32). Samples of UreABC—UreD—UreF—$UreG_{Str}$ or variants (10 μM nascent active site) were incubated in standard activation solution with varying amounts of Mg_2GTP. After 1 and 2 h, 100 μL aliquots were boiled for 5 min and centrifuged to pellet the precipitated protein; 90 μL of each supernatant was boiled and centrifuged again to remove more protein; and 80 μL of each supernatant was added to 20 μL of malachite green dye in a 96-well plate, mixed, and the absorbance monitored at 620 nm. The readings were compared to a standard curve prepared with known amounts of phosphate. Assays without protein were performed at each GTP concentration to control for GTP hydrolysis over time or at the higher temperatures.

RESULTS

Targets for site directed mutagenesis

K. aerogenes UreF residues were targeted for mutagenesis by using a previously published alignment (a greatly abbreviated alignment is depicted in supplementary material as Figure S1) of multiple UreF sequences (20) and the two available *H. pylori* UreF structures (15, 20). Many conserved residues lie close to the N- or C-termini, with the last 10 residues in the sequence showing high identity. Although residues 1–24 are unstructured in both *H. pylori* UreF crystal structures (15, 20), this has no consequence for *K. aerogenes* UreF which is shorter and lacks this N-terminal region. Mapping the highly conserved UreF residues onto the *H. pylori* crystal structure revealed a clustering on one face of the UreF dimer. (Of interest, the UreF residues at the interface between *H. pylori* UreF and UreH were poorly conserved and there is little overall sequence similarity between *K. aerogenes* UreD and *H. pylori* UreH). Based on the alignment and the structure, 16 *K. aerogenes* residues were chosen for mutagenesis to Ala (Figure 2). These included highly conserved residues near the N-terminus (P19, G21, Y23, S26, and E30), several residues at the C-terminus (H214, E215, R220, L221, F222, and S224), a few conserved potential hydrogen-bond forming residues in the middle (D60, E94 and Q171), one hydrophobic residue (F169), and the only lysine (K165) in the protein. A Lys or an Arg is present at this position in all known UreF sequences, and this positively-charged site is the best candidate for participating in an “Arg-finger”-like manner (33–35) to stimulate GTP hydrolysis in accord with the proposed GAP activity of UreF (21).

Mutants in *ureF* have variable effects on *in vivo* urease activity

E. coli cells expressing the complete urease operon, but encoding the selected variants of UreF, were shown by SDS-PAGE to produce levels of urease proteins that were essentially identical to those found with the wild-type accessory protein (data not shown). Cell-free extracts of these cultures were examined for urease activities and the results were shown to fall into three general categories (Figure 3 and Table S2). The mutant cells containing P19A, Y23A, E30A, E94A, H214A, R220A, L221A, F222A, and S224A forms of UreF all had less than 10% of the wild-type activity. These results highlight the critical *in vivo* role of the C-terminal region in urease activation, since altering any one of these highly conserved residues significantly decreased the urease activity. The mutant cells containing G21A, S26A, D60A, K165A, Q171A, and E215A UreF variants retained between 10 and 70% of the wild-type activity, indicating that they play important but not vital roles individually in the urease activation process. Finally, the mutant containing the F169A form of UreF exhibited wild-type activity, demonstrating the non-essentiality of this residue. The F169A variant of UreF was not characterized further.

UreF variants primarily affect binding of UreG in cell-free extracts

Using constructs that produce variant forms of UreE-F in the context of the other urease proteins, the fusion proteins were purified, along with accompanying proteins, from cell-free extracts by use of Ni-NTA resin. These samples were analyzed by SDS-PAGE (Figure 4A) and compared to the control sample where “pull-down” analysis of UreE-F resulted in substantial levels of co-purified UreABC, UreD, and, at lesser levels, UreG. Approximately equal levels of UreE-F were produced in all mutant cells according to the results from pull-down analysis as monitored by denaturing gel electrophoresis. The UreE-F protein containing the D60A substitution was not soluble and so the corresponding pull-down sample could not be analyzed. All other UreE-F pull-down samples, regardless of the changes within UreF, contained UreABC and UreD. This result provides confirmation of the proper folding of the UreE-F variants. UreG also remained bound to UreE-F versions containing S26A, Q171A, and E215A forms of UreF; notably, each of these UreF variants

resulted in cell-free extracts retaining at least 20% of wild-type activity. Surprisingly, the UreE-F samples corresponding to G21A and K165A UreF bound less UreG than control samples despite the relatively high levels of urease activity in cell-free extracts of these UreF variants (38 and 20% of wild-type UreF, respectively). The weaker interaction with UreG observed in these pull-down studies apparently could be overcome within the cellular milieu to allow substantial production of active enzyme, especially for the conservative G21A substitution. In contrast, UreG was greatly diminished or absent in pull-down samples from the P19A, Y23A, E30A, E94A, H214A, R220A, L221A, F222A, and S224A UreE-F variants; these results coincide with those for cell-free extracts of the corresponding UreF variants that exhibited <10% of wild type urease activity. Mapping these residues onto the UreF dimer, from the $(UreH—UreF)_2$ crystal structure (15), identified a clear binding pocket for UreG (yellow and magenta portions of Figure 5). These results highlight the importance of both the amino- and carboxyl-terminal residues of UreF for binding UreG.

UreF variants affect *in vitro* binding to $(UreABC—UreD)_3$ and $UreG_{Str}$

Prior studies had shown that $(UreABC—UreD)_3$ could bind, at low stoichiometry, to UreE-F according to pull-down studies using a Ni-NTA column (19). That work reported the purified UreE-F as being predominantly monomeric according to gel filtration chromatography; however, reevaluation of the native size by the same approach (in similar buffer conditions, but containing 100 mM NaCl rather than 200 mM NaCl) revealed the isolated protein to be primarily dimeric (~73 kDa), with a small amount of larger molecular weight aggregates. Each of the variant UreE-F proteins exhibited similar profiles, consistent with their presence as dimeric structures (and providing evidence for proper folding), except for D60A UreE-F that was insoluble and therefore not studied. Each purified UreE-F variant was combined with isolated $(UreABC—UreD)_3$, the mixtures were chromatographed on a Ni-NTA resin, and the extents of interaction between the proteins were analyzed by SDS-PAGE (an example using E30A UreE-F mixed with $(UreABC—UreD)_3$ is illustrated in Figure 4B) and quantified by gel scanning (Table 2). The original version of UreE-F bound $(UreABC—UreD)_3$ such that 0.32 UreC protomer was associated per UreE-F protomer, consistent with each $(UreE-F)_2$ dimer binding 0.21 $(UreABC—UreD)_3$ molecules under these conditions. The small amount of complex obtained in this *in vitro* study (using equivalent concentrations of UreE-F and UreABC—UreD incubated at room temperature for 20 min) is less than that observed for UreE-F pull-down studies from cell-free extracts (Figure 4A), consistent with cellular factors acting to enhance productive interaction. All the UreE-F variants except for the L221A variant bound less $(UreABC—UreD)_3$ than the fusion protein containing wild-type UreF; nevertheless, some interaction was retained in all cases. The P19A, G21A, and Y23A variants all bound about 70% of the amount of $(UreABC—UreD)_3$ compared to the original UreE-F, while the other UreE-F variants bound less than 50% of that bound by the control protein. These results demonstrate that none of the sites of substitution are essential for stabilizing the interaction between *K. aerogenes* UreF and $(UreABC—UreD)_3$, a result that is nicely compatible with the *H. pylori* $(UreH—UreF)_2$ structure (15).

An analogous series of studies was carried out by using *Strep*-tactin resin and $UreG_{Str}$ to examine the interactions of this protein with UreE-F and its variants. A representative gel depicting the interaction of $UreG_{Str}$ with the E30A variant of UreE-F is shown in Figure 4C and the measured ratios of protein binding for all variants are provided in Table 3. The *Strep*-tactin chromatography approach avoided the use of Ni, needed for the Ni-NTA resin, due to the known interaction between UreG and UreE in the presence of this metal ion (22). Interaction between $UreG_{Str}$ and UreE-F was maximized by incubating the mixture at 42 °C without NaCl prior to chromatography, resulting in 0.63 UreE-F protomer bound per $UreG_{Str}$. A much weaker interaction between these proteins was noted at 37 °C (data not

shown) and is consistent with UreD facilitating the UreE-F/UreG interaction in the pull-down studies from cell-free extracts, shown in Figure 4A. This *in vitro* interaction assay with its artificial conditions provided trends that substantially confirmed the results from UreE-F pull-down assays using cell-free extracts. $UreG_{Str}$ bound at least 75% of the S26A, Q171A, H214A, E215A, R220A, and S224A variant UreE-F proteins compared to control UreE-F. Similarly, 65–70% of control levels were found for P19A, Y23A, and F222A UreE-F, indicating only minor roles for those residues in stabilizing the binding between UreF and UreG. In contrast, the G21A, E30A, E94A, K165A, and L221A UreE-F variants exhibited substantially weaker binding (< 50% compared to control UreE-F) to $UreG_{Str}$. We conclude the residues associated with the latter positions are located at the UreF:UreG interface under these conditions, which represent only a subset of the interface residues when $(UreABC—UreD)_3$ is present as shown in Figure 4A.

Examination of UreF as a GTPase activating protein

In order to test the hypothesis that UreF acts as a GAP for UreG, several protein complexes containing UreF and UreG were tested for their GTPase activity by using a malachite green assay to detect product phosphate. First, UreE-F was incubated with $UreG_{Str}$ to examine whether the isolated proteins could stimulate GTPase activity (N.B., purified *K. aerogenes* UreG is essentially inactive (36)). Unfortunately, control assays using UreE-F alone revealed the presence of trace levels of contaminating GTPase in the protein preparation that was not eliminated by Ni-NTA or gel filtration chromatography, so this effort was halted since only UreG of the accessory proteins should have GTPase activity. The urease-free MBP-UreD—UreF—UreG complex (14, 29) also was investigated as a platform for testing the GAP hypothesis. This heterotrimeric complex appeared to possess GTPase activity; however, the complex containing the P-loop (T21A) variant of UreG, used as a negative control, also exhibited this activity. The assay result again indicated trace contamination by a GTPase so work on that complex was abandoned. As an alternate approach, studies were carried out with the previously described UreABC—UreD—UreF—$UreG_{Str}$ species (22) after performing an additional step of purification involving gel filtration chromatography.

UreABC—UreD—UreF—$UreG_{Str}$ and the complex containing the K165A UreF variant were purified (Figure 6A) for testing whether the highly conserved, positively-charged residue at position 165 functions like the Arg finger of a GAP (33–35). Consistent with the weakened binding of UreG in the K165A UreE-F pull-down studies utilizing cell-free extracts (Figure 4A), the complex prepared with the UreF variant possessed less $UreG_{Str}$ when examined after size exclusion chromatography. The complex also was prepared (gel not shown) using the T21A variant of $UreG_{Str}$ as a negative control that would be incapable of hydrolyzing GTP (10). Whereas the wild-type complex exhibited an initial increase in urease activity with increasing levels of GTP in the activation mixture, followed by a decrease in activation at greater GTP concentrations, the complex containing the T21A P-loop substitution in UreG resulted in decreasing extents of urease activation (possibly due to sequestration of Ni) with increasing GTP (Figure 6B). Significantly, the activities generated with these two complexes in the absence of GTP were similar. By contrast, the complex containing K165A UreF exhibited a decrease in activation competence with added GTP, but the overall level of urease activation was significantly greater than for the wild-type complex. Analogous activity patterns were obtained for samples subjected to activation for 2 h (data not shown); i.e., the complex formed with K165A UreF demonstrated greater activation competence in a GTP-independent manner compared to the wild-type complex (with or without GTP).

The extent of GTP hydrolysis for each urease activation sample was assessed after 1 h by using the malachite green assay (Figure 6C). The complex containing T21A UreG released little phosphate, with no further increase after 2 h of incubation, indicating the absence of

contaminating GTPase. The wild-type complex gave rise to an approximately linear increase in phosphate concentration with increasing amounts of GTP. At small GTP concentrations, the amount of phosphate formed was roughly proportional to the amount of active urease formed, but at concentrations greater than 75 μM GTP the amount of phosphate formed continued to increase while the activity diminished, consistent with an uncoupling of these processes. The complex containing K165A UreF possessed greater GTPase activity than the complex containing wild-type UreF at most GTP concentrations, demonstrating that K165 does not facilitate GAP activity. The comparatively large amount of phosphate produced by the variant complex also indicates that GTPase activity was significantly uncoupled from urease activation.

UreF functions to increase the fidelity of urease activation

The experiments described above demonstrate that a defective UreF enhances the GTPase activity of UreABC—UreD—UreF—UreG$_{Str}$ and cast doubt on the hypothesis that this protein serves as a GAP. Because the GTPase activity of the complex containing K165A UreF appears to be less coupled to urease activation than the complex of wild-type proteins, we hypothesize that UreF plays a non-GAP role; specifically, we propose that UreF is a gatekeeper that increases the fidelity of the activation process. Related to this notion, activation of the isolated urease apoprotein is known to generate activity in only ~15% of the nascent active sites even though the protein is fully metallated and carbamylation takes place (37, 38); thus, complete activation must somehow overcome the formation of the improperly formed metallocenters. Two experiments were carried out to explore the hypothesis that UreF enhances the fidelity of urease activation.

A time course activation experiment was performed in Ni-limiting conditions (i.e., 50 μM Ni versus 100 μM Ni, as used above) for the UreABC—UreD—UreF—UreG$_{Str}$ complex and the same complex containing K165A UreF, using activation assays with and without 75 μM Mg_2GTP (Figure 7). The resulting data were fitted to equation 1 to calculate maximal activities and the times needed to reach half-maximal activities. These fits ignored the possible slight diminishments in activation capacities for samples after incubation at 37 °C for 5 h. The complex containing K165A UreF activated quickly ($t_{1/2}$ 37 ± 12 min) and reached a maximal activity of 225 ± 16 U/mg. The presence of GTP led to slower activation ($t_{1/2}$ 77 ± 18 min) and a smaller final activity level (177 ± 14 U/mg), possibly due in part to chelation of Ni by GTP. In contrast, the wild-type complex was slow to activate whether GTP was absent or present ($t_{1/2}$ 83 ± 12 min and 80 ± 20 min, respectively), it formed little activity without GTP (118 ± 6 U/mg), and with GTP it reached approximately the same maximum activity (228 ± 19 U/mg) as observed for the complex containing K165A UreF in the absence of nucleotide. These results are compatible with the hypothesis that UreF enhances the efficiency of the process by improving the coupling to GTP hydrolysis, decreasing the rate of activation, and assuring the maximal amount of properly formed metallocenter.

As a more direct approach to evaluate this potential gatekeeper role of UreF, we assessed the effect of added Zn ions on the activation of UreABC—UreD—UreF—UreG$_{Str}$ containing wild-type and K165A accessory protein. Zn is known to compete effectively with Ni and hinder production of urease activity during activation of $(UreABC)_3$, $(UreABC\text{-}UreD)_3$, and $(UreABC\text{-}UreD\text{-}UreF)_3$ (7, 8, 38), but its effects on UreABC—UreD—UreF—UreG had never been examined. As illustrated in Figure 8, the presence of Zn in the activation mixture decreases the level of urease activity generated for both complexes studied whether or not GTP is present. The complexes were activated at three concentrations of Zn (0, 2.5, and 5.0 μM) and activities were measured at 1, 2, and 4 h to ensure maximal activation for analysis. After 2 h, both the wild-type and the K165A variant complexes had reached full activity according to the control assays without Zn, so that time point was analyzed. Whereas the

activity of complex containing wild-type UreF activated with GTP (solid black bar) was equivalent to the K165A UreF-containing complex (with or without GTP) in the absence of Zn (hatched and gray bars, respectively), the wild-type complex with GTP generated significantly more activity ($p < 0.05$) than the other mixtures in the presence of low concentrations of Zn. These results indicate that wild-type UreF allows the GTPase activity of UreG to partially protect against improper metallocenter assembly. UreF thus plays an important role in coupling the GTPase activity to urease activation, insuring proper di-Ni cluster formation.

DISCUSSION

This study has significantly enhanced our understanding of the UreF urease accessory protein by clarifying its interactions with UreG and its role in urease activation. Prior efforts had shown that free *K. aerogenes* UreF is insoluble (8) whereas a truncated version of the *H. pylori* protein is soluble and was structurally defined (20). In addition, soluble forms of UreF are known to be found in various complexes including $(UreH—UreF)_2$ from *H. pylori* (15) and the following *K. aerogenes* species: MBP-UreD—UreF—UreG (14), $(UreABC—UreD—UreF)_3$ (8), and UreABC—UreD—UreF—UreG (9). The $(UreH—UreF)_2$ structure defined how UreF interacts with the UreD homologue and mutational studies in the same work provided evidence that Y48 and R250 in the *H. pylori* UreF protein (corresponding to Y23 and R220 in *K. aerogenes* UreF) are critical for binding UreG (15); however, other specific residues involved in UreG binding were not defined. There is no crystal structure available for any UreG sample, perhaps because the isolated protein cannot be crystallized due to its intrinsic disorder according to NMR, circular dichroism, and fluorescence spectroscopic analyses (39, 40), so modeling of UreF/UreG interaction (15) can provide only a crude notion of the potential interface surfaces. The present investigations extend knowledge of residues critical to this interface and provide new experimental insights into the role of UreF in urease activation.

The current study targeted sixteen highly conserved UreF residues for mutagenesis as a means to identify their importance in urease activation and UreG binding. Urease assays of cell-free extracts from cultures containing the complete urease gene cluster showed that nine of the mutant cells exhibited less than 10% of the wild type activity, including those producing the Y23A and R220A UreF variants (comparable to the two *H. pylori* UreF variants mentioned above), confirming their importance in urease activation. UreE-F pull-down assays using cell-free extracts showed that substitutions affecting each of these nine residues had reduced levels of UreG binding, with six leading to the absence of associated UreG. The G21A and K165A variants had somewhat greater urease activity (38 and 20 U/mg, respectively), but also had reduced amounts of UreG. These important residues map to a 1300 $Å^2$ surface on UreF (Figure 5), and are close to the binding surface for UreD, consistent with how the three proteins are known to work together for urease activation. None of the site-directed mutations greatly affected the interaction between UreF and UreABC—UreD, as expected on the basis of the $(UreH—UreF)_2$ crystal structure which showed that only one of the highly conserved residues we chose to mutate (E215) is located at the UreD binding surface. It is intriguing that the UreG binding site on UreF has so many highly conserved residues, whereas the UreD and urease binding sites on this protein are not highly conserved. Possibly related to this finding, UreG is the most highly conserved urease accessory protein whereas alignments of UreD or UreF proteins each exhibit significantly less similarity.

We attempted to directly test the proposed role of UreF as a GAP (21) by comparing the activation properties of UreABC—UreD—UreF—$UreG_{Str}$ complexes containing wild-type and K165A UreF. K165 is the only Lys in *K. aerogenes* UreF and this position is always

occupied by a Lys or Arg residue in homologues; thus, this positively-charged residue could reasonably correspond to the typical Arg finger motif that is found in GAP proteins (33–35). The Arg finger of GAPs plays a dual role in generating the nucleophilic water molecule needed for hydrolysis and stabilizing the transition state (34). Urease assays using cell-free extracts showed that K165 of UreF plays a non-essential role in urease activation, with 20% of the wild-type urease activity retained when using a culture that synthesizes K165A UreF along with the other urease proteins. *In vitro* assays using wild-type and variant UreABC—UreD—UreF—UreG$_{Str}$ complexes unexpectedly demonstrate that the species containing K165A UreF results in enhanced levels of urease activity. We don't have a simple explanation for why the *in vivo* and *in vitro* results differ in this manner; however, we note that the urease activation conditions are quite distinct for these two processes. For the purified complex, activation of the K165A UreF-containing version is inhibited, not enhanced, by GTP, unlike the control complex. More significantly, the variant complex exhibits greater GTPase activity than the wild-type complex; thus ruling out the possibility that K165 serves in the Arg finger role of a GAP. Although K165 does not function as an Arg finger, it remains possible that R220, another highly conserved and positively-charged residue (in this case near the critically important C-terminus), could serve in this manner. Our UreE-F pull-down assays using cell-free extracts reveal the lack of UreG binding to the complex containing the R220A variant of UreE-F, so it was not possible to test the effect of mutating this residue in UreABC—UreD—UreF—UreG$_{Str}$ as was accomplished with the K165A UreF variant. If R220 could act as an Arg finger, one would need to postulate that K165 modulates its effect so that the K165A variant leads to greater GTPase activity. There are examples of GAP-GTPase interactions that do not involve an Arg finger, for example the Rap-RapGAP complex (41, 42). Nevertheless, the above studies greatly reduce the possibility that UreF acts as a GAP, thus encouraging us to consider and test other hypotheses for its function.

The finding that UreABC—UreD—UreF—UreG$_{Str}$ activation is less coupled to GTPase activity when using K165A UreF and the demonstration of increased urease activity resulting from the substituted version of UreF led us to consider a gatekeeper role for this protein; i.e., UreF would help to ensure proper metallocenter assembly during urease activation. The complexes with the two forms of UreF have the same final activation competence, but that containing wild-type protein requires GTP while that with K165A UreF is inhibited by the nucleotide. The time course assays reveal a more rapid activation of the K165A UreF-containing complex (lacking GTP) than noted in the complex with wild-type UreF (with or without GTP), consistent with wild-type UreF hindering the rate of activation while insuring greater fidelity of metallocenter biosynthesis. In contrast, the K165A variant allowed the process to occur more quickly but possibly with less control. UreG's GTPase activity appears to play a role in controlling the rate of activation, and when this activity is uncoupled from activation (i.e., when using K165A UreF) urease activity is generated much faster. It is likely more important that the timing is tightly regulated in the cell compared to the idealized environment of the test tube, since the K165A variant only has 20% of the wild type activity *in vivo*. The GTPase activity could play a role in gating the timing of the Ni transfer to the active site in order to prevent the metal from binding incorrectly (as in the 85% of the urease apoprotein that becomes carbamylated and binds Ni, yet remains inactive when subjected to activation conditions as mentioned earlier). This hypothesis is supported by the demonstration that the complex formed with wild-type UreF (coupled to GTPase activity) is more resistant to inhibition by Zn during activation than is the case for the variant complex. We propose that UreF induces a conformational change in, or stabilizes the structure of, UreG that allows for the latter protein's hydrolytic capacity while ensuring a tight coupling between GTP hydrolysis and proper metal assembly. Replacing K165 with Ala leads to greater uncoupling of the activation and hydrolysis steps, thus yielding enhanced rates of activation under favorable conditions, but allowing incorrect

metal assembly when Zn is present, and possibly having additional negative consequences *in vivo*. This model is compatible with the finding that GTPase activity is not essential *in vitro* for partial activation, as has long been known for $(UreABC)_3$, $(UreABC—UreD)_3$, and $(UreABC—UreD—UreF)_3$ (8, 9, 38), but the full set of accessory proteins allows for greater final levels of activation to occur with UreF increasing the fidelity of the process. Thus, when all urease accessory proteins, including UreE, are present, urease can be activated fully (11).

The suggestion that GTPase activity can be used as a checkpoint has been reported for other proteins in the same family as UreG. For example, the GTPase activity of HypB, a protein that functions in hydrogenase maturation in *E. coli*, is thought to gate Ni transfer into hydrogenase with the participation of the Ni-binding protein SlyD (43). Similarly, MeaB, another member of the small GTPase family, serves a gating function for incorporating coenzyme B_{12} into methylmalonyl-CoA mutase (44). We propose that UreF works to improve the coupling of UreG's GTPase activity to Ni insertion into urease.

In conclusion, we have confirmed that mutations affecting a series of highly conserved UreF residues have dramatic effects on *in vivo* urease activity. Using these same UreF variants in UreE-F pull-down assays with cell extracts or by carrying out interaction studies with purified UreF and UreG components, we have identified several UreF residues that make up the binding surface for UreG. We have also evaluated a proposed role of UreF as a GAP and obtained no evidence to support this hypothesis since a variant UreF gave rise to increased GTPase activity. Finally, we provide evidence that UreF is needed for coupling GTPase activity to ensure proper metallocenter assembly, where the gating function of UreF increases the fidelity of activation—especially when competing Zn is present.

Supplementary Material

Refer to Web version on PubMed Central for supplementary material.

Acknowledgments

We thank Brittnie DeVries for her assistance with mutagenesis and lab members for helpful discussions.

Abbreviations

$(UreABC)_3$	urease apoprotein
DTT	dithiothreitol
GAP	GTPase activating protein
HEPES	4-(2-hydroxyethyl)-1-piperazineethanesulfonic acid
IPTG	isopropyl β-D-1-thiogalactopyranoside
MBP	maltose binding protein
NTA	nitrilotriacetic acid
PAGE	polyacrylamide gel electrophoresis
SAXS	small-angle x-ray scattering
SDS	sodium dodecyl sulfate
TCEP	tris(2-carboxyethyl)phosphine
UreE-F	translational fusion of UreE and UreF

UreG$_{Str}$ UreG tagged with *Strep II*

References

1. Mobley HLT, Island MD, Hausinger RP. Molecular biology of microbial ureases. Microbiol Rev. 1995; 59:451–480. [PubMed: 7565414]
2. Carter EL, Flugga N, Boer JL, Mulrooney SM, Hausinger RP. Interplay of metal ions and urease. Metallomics. 2009; 1:207–221. [PubMed: 20046957]
3. Witte CP. Urea metabolism in plants. Plant Science. 2011; 180:431–438. [PubMed: 21421389]
4. Zambelli B, Musiani F, Benini S, Ciurli S. Chemistry of Ni^{2+} in urease: sensing, trafficking, and catalysis. Accounts of Chemical Research. 2011; 44:520–530. [PubMed: 21542631]
5. Jabri E, Carr MB, Hausinger RP, Karplus PA. The crystal structure of urease from *Klebsiella aerogenes*. Science. 1995; 268:998–1004. [PubMed: 7754395]
6. Lee MH, Mulrooney SB, Hausinger RP. Purification, characterization, and *in vivo* reconstitution of *Klebsiella aerogenes* urease apoenzyme. J Bacteriol. 1990; 172:4427–4431. [PubMed: 2142939]
7. Park IS, Carr MB, Hausinger RP. *In vitro* activation of urease apoprotein and role of UreD as a chaperone required for nickel metallocenter assembly. Proc Natl Acad Sci USA. 1994; 91:3233–3237. [PubMed: 7909161]
8. Moncrief MBC, Hausinger RP. Purification and activation properties of UreD-UreF-urease apoprotein complexes. J Bacteriol. 1996; 178:5417–5421. [PubMed: 8808930]
9. Park IS, Hausinger RP. Evidence for the presence of urease apoprotein complexes containing UreD, UreF and UreG in cells that are competent for *in vivo* enzyme activation. J Bacteriol. 1995; 177:1947–1951. [PubMed: 7721685]
10. Soriano A, Hausinger RP. GTP-dependent activation of urease apoprotein in complex with the UreD, UreF, and UreG accessory proteins. Proc Natl Acad Sci USA. 1999; 96:11140–11144. [PubMed: 10500143]
11. Soriano A, Colpas GJ, Hausinger RP. UreE stimulation of GTP-dependent urease activation in the UreD-UreF-UreG-urease apoprotein complex. Biochemistry. 2000; 39:12435–12440. [PubMed: 11015224]
12. Quiroz-Valenzuela S, Sukuru SCK, Hausinger RP, Kuhn LA, Heller WT. The structure of urease activation complexes examined by flexibility analysis, mutagenesis, and small-angle X-ray scattering. Arch Biochem Biophys. 2008; 480:51–57. [PubMed: 18823937]
13. Chang ZZ, Kuchar J, Hausinger RP. Chemical cross-linking and mass spectrometric identification of sites of interaction for UreD, UreF, and urease. J Biol Chem. 2004; 279:15305–15313. [PubMed: 14749331]
14. Carter EL, Hausinger RP. Characterization of *Klebsiella aerogenes* urease accessory protein UreD in fusion with the maltose binding protein. J Bacteriol. 2010; 192:2294–2304. [PubMed: 20207756]
15. Fong YH, Wong HC, Chuck CP, Chen YW, Sun H, Wong KB. Assembly of preactivation complex for urease maturation in *Helicobacter pylori*. J Biol Chem. 2011; 286:43241–43249. [PubMed: 22013070]
16. Heimer SR, Mobley HLT. Interaction of *Proteus mirabilis* urease apoenzyme and accessory proteins identified with yeast two-hybrid technology. J Bacteriol. 2001; 183:1423–1433. [PubMed: 11157956]
17. Rain JC, Selig L, De Reuse H, Battaglia V, Reverdy C, Simon S, Lenzen G, Petel F, Wojcik J, Schachter V, Chemama Y, Labigne AS, Legrain P. The protein-protein interaction map of *Helicobacter pylori*. Nature. 2001; 409:211–215. [PubMed: 11196647]
18. Kim KY, Yang CH, Lee MH. Expression of the recombinant *Klebsiella aerogenes* UreF protein as a MalE fusion. Arch Pharm Res. 1999; 22:274–278. [PubMed: 10403130]
19. Kim JK, Mulrooney SB, Hausinger RP. The UreEF fusion protein provides a soluble and functional form of the UreF urease accessory protein. J Bacteriol. 2006; 188:8413–8420. [PubMed: 17041056]

20. Lam R, Romanov V, Johns K, Battaile KP, Wu-Brown J, Guthrie JL, Hausinger RP, Pai EF, Chirgadze NY. Crystal structure of a truncated urease accessory protein UreF from *Helicobacter pylori*. Proteins. 2010; 78:2839–2848. [PubMed: 20635345]
21. Salomone-Stagni M, Zambelli B, Musiani F, Ciurli S. A model-based proposal for the role of UreF as a GTPase-activating protein in the urease active site biosynthesis. Proteins. 2007; 68:749–761. [PubMed: 17510959]
22. Boer JL, Quiroz-Valenzuela S, Anderson KL, Hausinger RP. Mutagenesis of *Klebsiella aerogenes* UreG to probe nickel binding and interactions with other urease-related proteins. Biochemistry. 2010; 49:5859–5869. [PubMed: 20533838]
23. Zambelli B, Turano P, Musiani F, Neyroz P, Ciurli S. Zn^{2+}-linked dimerization of UreG from *Helicobacter pylori*, a chaperone involved in nickel trafficking and urease activation. Proteins. 2009; 74:222–239. [PubMed: 18767150]
24. Zambelli B, Stola M, Musiani F, De Vriendt K, Samyn B, Devreese B, Van Beeumen J, Turano P, Dikiy A, Bryant DA, Ciurli S. UreG, a chaperone in the urease assembly process, is an intrinsically unstructured GTPase that specifically binds Zn^{2+} J Biol Chem. 2005; 280:4684–4695. [PubMed: 15542602]
25. Zambelli B, Musiani F, Savini M, Tucker P, Ciurli S. Biochemical studies on *Mycobacterium tuberculosis* UreG and comparative modeling reveal structural and functional conservation among the bacterial UreG family. Biochemistry. 2007; 46:3171–3182. [PubMed: 17309280]
26. Colpas GJ, Brayman TG, Ming LJ, Hausinger RP. Identification of metal-binding residues in the *Klebsiella aerogenes* urease nickel metallochaperone, UreE. Biochemistry. 1999; 38:4078–4088. [PubMed: 10194322]
27. Bellucci M, Zambelli B, Musiani F, Turano P, Ciurli S. *Helicobacter pylori* UreE, a urease accessory protein: specific Ni^{2+}- and Zn^{2+}-binding properties and interaction with its cognate UreG. Biochem J. 2009; 422:91–100. [PubMed: 19476442]
28. Miroux B, Walker JE. Over-production of proteins in *Escherichia coli*: Mutant hosts that allow synthesis of some membrane proteins and globular proteins at high levels. J Mol Biol. 1996; 260:289–298. [PubMed: 8757792]
29. Carter EL, Boer JL, Farrugia MA, Flugga N, Towns CL, Hausinger RP. The function of UreB in *Klebsiella aerogenes* urease. Biochemistry. 2011; 50:9296–9308. [PubMed: 21939280]
30. Laemmli UK. Cleavage of structural proteins during assembly of head of bacteriophage-T4. Nature. 1970; 227:680. [PubMed: 5432063]
31. Weatherburn MW. Phenol-hypochlorite reaction for determination of ammonia. Anal Chem. 1967; 39:971–974.
32. Baykov AA, Evtushenko OA, Avaeva SM. A malachite green procedure for orthophosphate determination and its use in alkaline phosphatase-based enzyme immunoassay. Anal Biochem. 1988; 171:266–270. [PubMed: 3044186]
33. Ahmadian MR, Stege P, Scheffzek K, Wittinghofer A. Confirmation of the arginine-finger hypothesis for the GAP-stimulated GTP-hydrolysis reaction of Ras. Nature Struct Biol. 1997; 4:686–689. [PubMed: 9302992]
34. Resat H, Straatsma TP, Dixon DA, Miller JH. The arginine finger of RasGAP helps Gln-61 align the nucleophilic water in GAP-stimulated hydrolysis of GTP. Proc Natl Acad Sci. 2001; 98:6033–6038. [PubMed: 11371635]
35. Scheffzek K, Ahmadian MR. GTPase activating proteins: structural and functional insights 18 years after discovery. Cell Mol Life Sci. 2005; 62:3014–3038. [PubMed: 16314935]
36. Moncrief MBC, Hausinger RP. Characterization of UreG, identification of a UreD-UreF-UreG complex, and evidence suggesting that a nucleotide-binding site in UreG is required for in vivo metallocenter assembly of *Klebsiella aerogenes* urease. J Bacteriol. 1997; 179:4081–4086. [PubMed: 9209019]
37. Park IS, Hausinger RP. Requirement of carbon-dioxide for *in vitro* assembly of the urease nickel metallocenter. Science. 1995; 267:1156–1158. [PubMed: 7855593]
38. Park IS, Hausinger RP. Metal ion interactions with urease and UreD-urease apoproteins. Biochemistry. 1996; 35:5345–5352. [PubMed: 8611523]

39. Neyroz P, Zambelli B, Ciurli S. Intrinsically disordered structure of *Bacillus pasteurii* UreG as revealed by steady-state and time-resolved fluorescence spectroscopy. Biochemistry. 2006; 45:8918–8930. [PubMed: 16846235]

40. Zambelli B, Cremades N, Neyroz P, Turano P, Uversky VN, Ciurli S. Insights in the (un)structural organization of *Bacillus pasteurii* UreG, an intrinsically disordered GTPase enzyme. Mol Biosyst. 2012; 8:220–228. [PubMed: 21922108]

41. Chakrabarti PP, Suveyzdis Y, Wittinghofer A, Gerwert K. Fourier transform infared spectroscopy on the Rap-RapGAP reaction, GTPase activation without an arginine finger. J Biol Chem. 2004; 279:46226–26233. [PubMed: 15292263]

42. Scrima A, Thomas C, Deaconescu D, Wittinghofer A. The Rap-RapGAP complex: GTP hydrolysis without catalytic glutamine and arginine residues. EMBO J. 2008; 27:1145–1153. [PubMed: 18309292]

43. Kaluarachchi H, Zhang JW, Zamble DB. *Escherichia coli* SlyD, more than a Ni(II) reservoir. Biochemistry. 2011; 50:10761–10763. [PubMed: 22085337]

44. Padovani D, Banerjee R. A G-protein editor gates coenzyme B-12 loading and is corrupted in methylmalonic aciduria. Proc Natl Acad Sci USA. 2009; 106:21567–21572. [PubMed: 19955418]

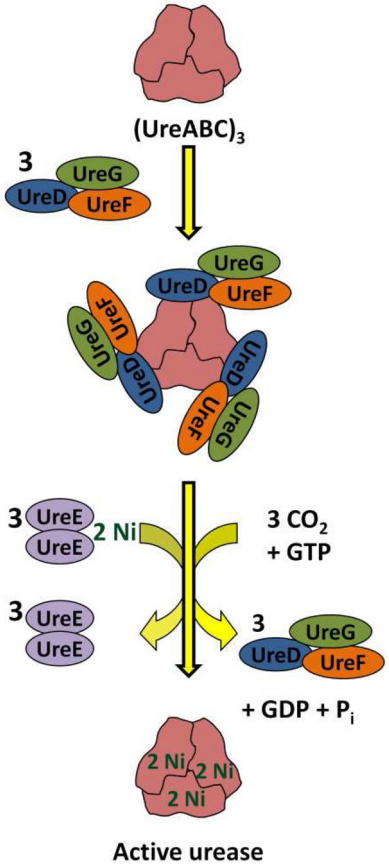

Figure 1.

Simplified scheme of the urease activation process. Urease is synthesized as an apoprotein, lacking Ni ions and with its active site Lys free of carbamylation. Accessory proteins UreD, UreF, and UreG bind to the apoprotein and, through a process not completely understood, the Lys is carbamylated by CO_2, the metallochaperone UreE delivers Ni, GTP is hydrolyzed, and the auxiliary proteins depart leaving active urease.

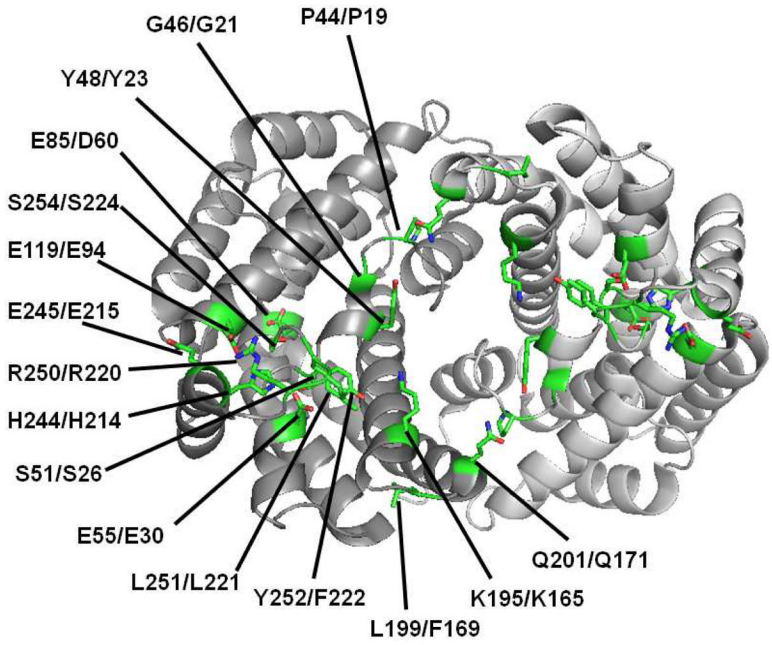

Figure 2.
Mutagenesis of *K. aerogenes* UreF. The structure depicted is that of *H. pylori* UreF, from the (UreH—UreF)$_2$ complex (PDB code 3SF5), with the protomers colored in two shades of gray and the residues changed to alanine in the *K. aerogenes* protein shown in green and identified with the *H. pylori* residue number/*K. aerogenes* residue number.

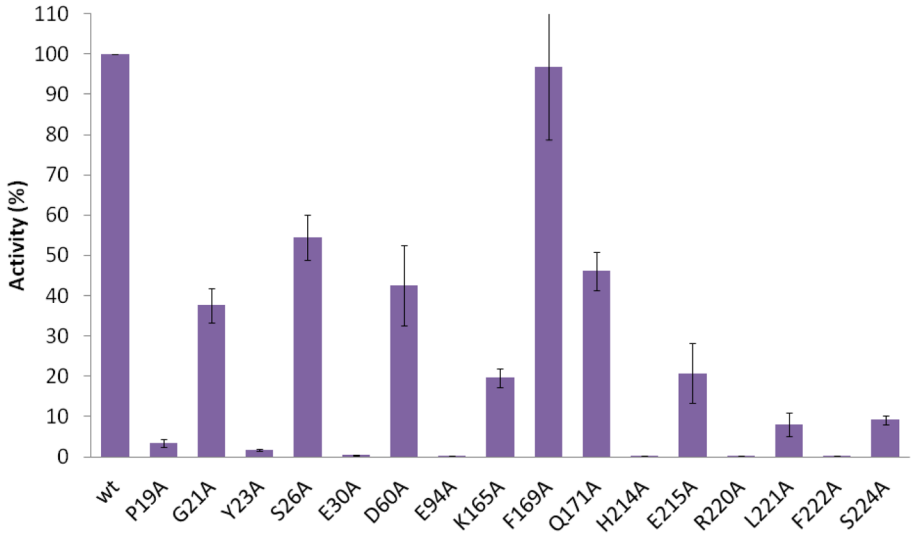

Figure 3.

Effect of UreF variants on urease activity in cell-free extracts. Percent activity values shown are relative to that of cell-free extracts of cells containing the wild-type urease gene cluster. Measured urease specific activities are provided in Table S2.

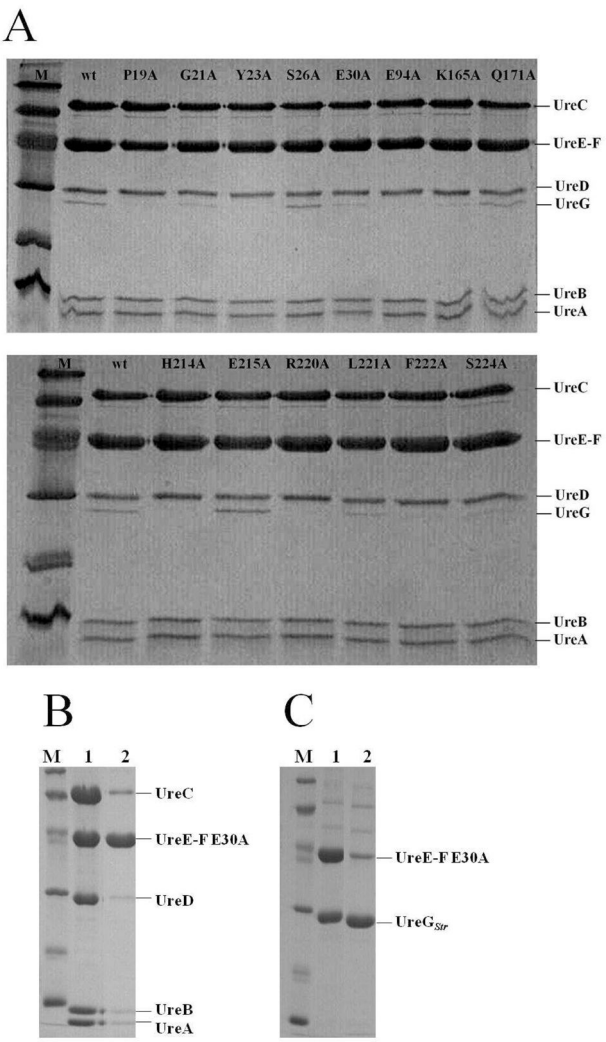

Figure 4.

Pull-down assays. A. UreE-F pull-down analyses of cell-free extracts identify UreF mutations that lead to reduction or absence of UreG binding. Extracts of cells containing pKKEF, bearing the complete *ure* cluster with *ureE* and *ureF* fused (along with its *ureF* variants), were added to Ni-NTA resin, washed, and eluted with 1 M imidazole. Eluted fractions were analyzed by SDS-PAGE using a 15% acrylamide gel. B. Pull-down assay for UreE-F mixed with (UreABC—UreD)$_3$. In this example, E30A UreE-F was mixed with (UreABC—UreD)$_3$ (lane 1) then bound to Ni-NTA resin and eluted, along with any associated proteins, by addition of imidazole (lane 2). C. Pull-down assay for UreG$_{Str}$ mixed with UreE-F. In this example, UreG$_{Str}$ was mixed with E30A UreE-F (lane 1) then bound to *Strep*-tactin resin and eluted, along with any associated proteins, by addition of desthiobiotin (lane 2). For each panel, the lane labeled M denotes the marker proteins (97.4, 66, 45, 31, 21.5, and 14.4 kDa).

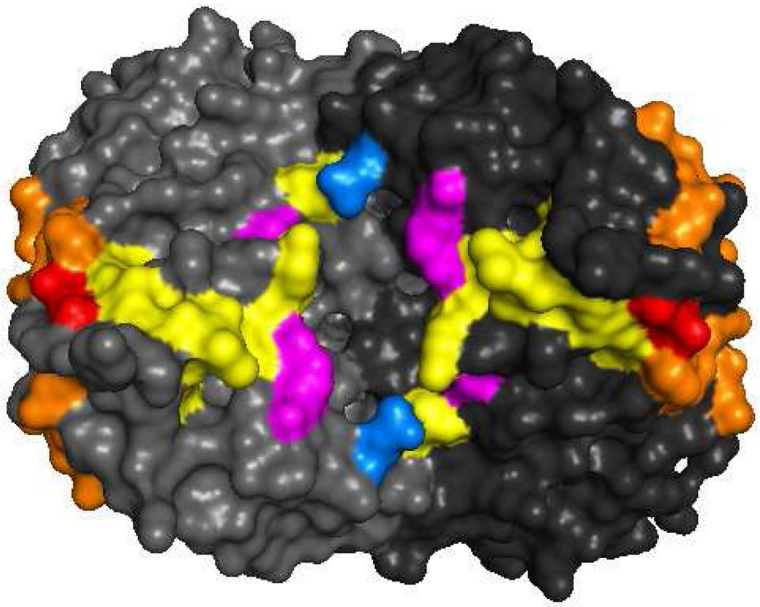

Figure 5.

UreF mutations affecting UreG binding. The two protomers of *H. pylori* UreF are shown in different shades of grey in space fill mode (PDB code 3SF5). Residues are colored to indicate the corresponding side chains of *K. aerogenes* UreF where mutation to Ala had no effect on UreG binding (blue), mutations resulting in low levels of UreG binding and <10% urease activity (yellow), mutations causing reduced UreG binding but retention of >10% urease activity (magenta), and mutation leading to only 21% activity but retention of UreG binding (red). Residues that interact with UreH in *H. pylori* are colored orange or red.

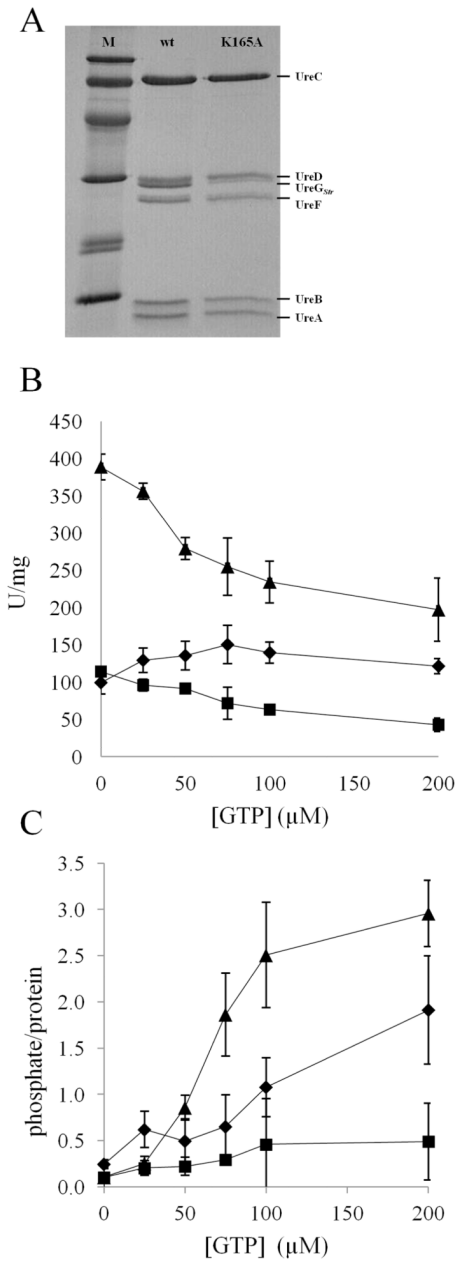

Figure 6.

Effect of K165A UreF on GTP-dependent activation and phosphate release by UreABC—UreD—UreF—UreG$_{Str}$. (A) SDS-PAGE analysis of UreABC—UreD—UreF—UreG$_{Str}$ and UreABC—UreD—UreF(K165A)—UreG$_{Str}$ after purification by affinity resin and gel filtration chromatography. M denotes the marker proteins (97.4, 66, 45, 31, 21.5, and 14.4 kDa). (B) Urease activation assays for versions of UreABC—UreD—UreF—UreG$_{Str}$. Proteins (10 μM) were incubated for one h at 37 °C in standard activation solution with the indicated concentrations of Mg_2GTP. Aliquots were removed and assayed for urease activity. (C) Phosphate released by UreABC—UreD—UreF—UreG$_{Str}$ during activation as in (B). Symbols used in (B) and (C): UreABC—UreD—UreF—UreG$_{Str}$ with wild-type UreF (◆), K165A UreF (▲), or T21A UreG$_{Str}$ (■).

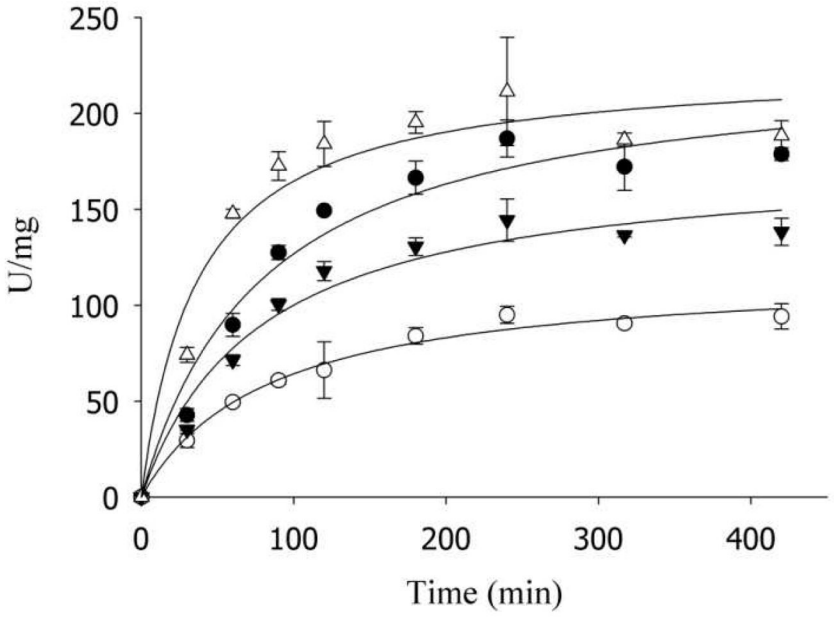

Figure 7.

Comparison of activation time course for UreABC—UreD—UreF—UreG$_{Str}$ complex and UreABC—UreD—UreF(K165A)—UreG$_{Str}$. Proteins (0.5 μM) were incubated in standard activation buffer except for only containing 50 μM Ni. The wild–type and K165A complexes were incubated in the absence (○ and △, respectively) or the presence (● and ▼, respectively) of 75 μM Mg_2GTP. Fits using equation 1 are shown for each data set.

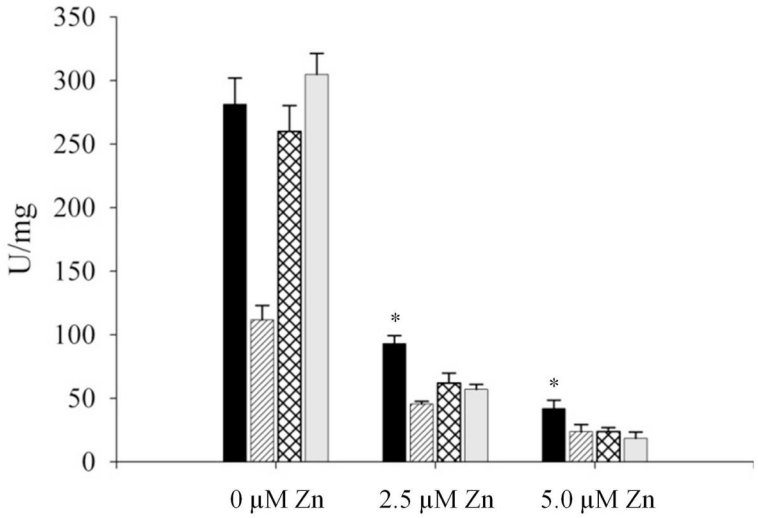

Figure 8.

Zn inhibition of UreABC—UreD—UreF—UreG$_{Str}$ (0.5 μM) activation under standard conditions for complexes containing wild-type and K165A UreF. Protein complexes (0.5 μM) were incubated for two h at 37 °C in standard activation solution with the indicated concentrations of $ZnSO_4$. The wild-type and K165A complexes were incubated in the presence (black and hatched, respectively) or absence (diagonal and grey, respectively) of 75 μM Mg_2GTP. The asterisks indicate statistically significant differences ($p < 0.05$) of the sample indicated versus the samples subjected to the same conditions.

Table 1

Plasmid properties

Plasmid	Description	Reference
pKK17	Wild-type *K. aerogenes* urease cluster (*ureDABCEFG*) inserted into pKK223-3	(26)
pKK17-P19A, -G21A, -Y23A, -S26A, -E30A, -D60A, -E94A, -K165A, -F169A, -Q171A, -H214A, -E215A, -R220A, - L221A, -F222A, -S224A	Single site mutations of pKK17 for studying the effects of the encoded UreF variants on urease activity	This study
pKKEF	Same as pKK17, but with a translational fusion of UreE and UreF	This study
pKKEF-P19A, -G21A, -Y23A, -S26A, -E30A, -D60A, -E94A, -K165A, -F169A, -Q171A, -H214A, -E215A, -R220A, - L221A, -F222A, -S224A	Single site mutations of pKKEF for *in vivo* pull- down studies using the encoded proteins	This study
pET-EF	Translationally fused *ureEF* genes inserted into pET21 for production of the UreE-F fusion protein	(19)
pET-EF-P19A, -G21A, -Y23A, -S26A, -E30A, -D60A, -E94A, -K165A, -F169A, -Q171A, -H214A, -E215A, -R220A, - L221A, -F222A, -S224A	Single site mutations of pET-EF for production of UreE-F variants for *in vitro* pull-down studies	This study
pKKG	Same as pKK17, but with a translational fusion of UreG and a *Strep II* tag	(22)
pKKG-UreF-K165A	Single site mutation of pKKG encoding the K165A UreF variant	This study
pKKG-T21A	Single site mutation of pKKG encoding the T21A variant of *Strep II* tagged UreG	This study
pEC005	*ureFG* fragment cloned into pACT3 for production of UreF and UreG	(14)
pEC005-UreF-K165A	Single site mutation of pEC005 that encodes the K165A variant of UreF along with UreG	This study
pEC005-UreG-T21A	Single site mutation of pEC005 that encodes the T21A variant of UreG along with UreF	This study
pKAUD2	Plasmid for production of $(UreABC—UreD)_3$	(7)
pIBA3+UreG	pASK-IBA3plus-derived plasmid for production of UreG with a *Strep II* tag fused to its C-terminus	(22)
pEC002	*ureD* cloned into pMal-c2x for production of UreD fused at its C-terminus to MBP. Used along with pEC005 for production of MBP-UreD—UreF—UreG.	(14)

Table 2

Binding of UreABC—UreD by control and variant UreE-F samples[a]

UreE-F variant	Ratio of UreABC—UreD/UreE-F
Wild-type	0.32
P19A	0.21
G21A	0.22
Y23A	0.22
S26A	0.15
E30A	0.13
E94A	0.05
K165A	0.14
Q171A	0.13
H214A	0.05
E215A	0.13
R220A	0.11
L221A	0.34
F222A	0.15
S224A	0.08

[a]Determined by *in vitro* pull-down studies with Ni-NTA and gel scanning comparison of bands for UreC and UreE-F. On the basis of replicate measurements for selected samples, the typical standard deviations in the ratio are approximately 0.10.

Table 3

Binding of control and variant UreE-F by $UreG_{Str}$[a]

UreE-F variant	Ratio of UreE-F/$UreG_{Str}$
Wild-type	0.63
P19A	0.42
G21A	0.30
Y23A	0.43
S26A	0.54
E30A	0.18
E94A	0.28
K165A	0.26
Q171A	0.55
H214A	0.50
E215A	0.49
R220A	0.55
L221A	0.25
F222A	0.42
S224A	0.52

[a]Determined by *in vitro* pull-down studies using *Strep*-tactin resin and gel scanning